

SUPERNOVAE EXPLOSIONS THEORY AND COMPACT REMNANT OF SN 1987A

V.M. Chechetkin¹, A.A. Baranov², M.V. Popov^{1,2}, A.Yu. Lugovsky¹

¹ Keldysh Institute of Applied Mathematics,

Russian Academy of Science, Miusskay sq. 4, 125047, Moscow, Russia.

² Laboratoire d'Annecy-le-Vieux de Physique Theorique (LAPTH), Université de Savoie,
9, Chemin de Bellevue BP 110, 74941 Annecy-le-Vieux Cedex, France.

mikhail.v.popov@gmail.com

ABSTRACT. Hydrodynamics of massive star explosion within a non-spherical supernova model is presented. The explosive burning is computed in the *He*-core of a progenitor. It is assumed that the iron core and the other layers of the intermediate-mass nuclei formed a compact central object beyond the mass cut and its formation did not disturb the stellar envelope. A Piecewise Parabolic Method on a Local stencil (PPML) is applied to simulate the hydrodynamics of the explosion. The problem of compact remnant creation after the explosion is discussed in relation with SN 1987A observations. The computations show that at the neighbourhood of compact remnant a significant quantity of the matter should remain. The accretion of this matter to the compact remnant should produce strong radiation which is not observed in the case of SN 1987A.

Key words: hydrodynamics, PPML; supernovae, compact remnant, accretion, SN 1987A.

1. Introduction

As is well known there are two classes of supernovae (SNe) with different mechanisms of explosion – thermonuclear SNe (type Ia), with the white dwarfs progenitors, and core-collapse SNe (type II, Ib/c) with the massive stars progenitors. The theory of SNe involves a large number of fundamental problems of modern physics and astrophysics which are not solved yet. Although the explosion mechanisms are completely different, the large-scale convective processes and hydrodynamic instabilities play a very important role in both cases (Ustyugov et al. 1999, Popov et al. 2004, Bychkov et al. 2006). In this paper we discuss the hydrodynamic of massive star explosion by an example of non-spherical model and the problem of compact remnant after the explosion in relation with SN 1987A observations.

For our hydrodynamic model of core-collapse SN we

have chosen the parameters of a Population I metal rich $25 M_{\odot}$ star. We have assumed that by the explosion moment the inner part of the star collapsed and produced $\sim 10^{52}$ ergs. Assuming that the size of this collapsed part is small in comparison with the size of *He*-envelope, we start the hydrodynamic computations of propagation of the shock through the *He*-envelope. The explosion is initiated by inserting the energy into the central part of the star and distributing it in an asymmetric way. So we assume a jet-like structure of the explosion when the ejected matter preferentially moves along the rotational axis. This kind of asymmetry could be explained by acting of Archimedes' force on the hot and light products of explosive burning. In the case of rotation the levels of constant density have a form, similar to ellipsoids of rotation, making the steepest pressure gradient along the axis. It means that the Archimedes' force is acting along this direction. This mechanism requires time to deform the shape of the burnt matter, extending it along the axis. Here we must assume the deflagration regime of burning when at the initial stage the burning front propagates with subsonic velocity. In this case a hot core disintegrates forming two large-scale convective bubbles which are floating up and down. As a result this should produce a jet-like structure of the explosion. The dynamics of such bubbles was studied, for example, in (Bychkov et al. 2006). Also the acting of magnetic fields favours a jet-like structure, see for example the magnetorotational mechanism of SN (Moiseenko et al. 2010).

A theoretical reason for the axisymmetric explosion could be an assumption of the deflagration regime of nuclear burning in the stellar core under the conditions of hydrostatic equilibrium for SNe type Ia and nonequilibrium neutronization of the matter in the central part of the protoneutron star for SNe type II, Ib/c. For SNe type Ia formation of large-scaled bubbles is the first stage of explosion, after which the deflagration flame could transform to a detonation regime. This is a delayed detonation scenario (deflagration-detonation

transition) (Ivanova et al. 1974, Khokhlov 1991).

One of the main problems in the theory of SNe II is to show how a neutron star is born in the explosion. During the gravitational collapse of the iron core of a massive star, huge energy is released in the form of neutrinos. However, these neutrinos remain trapped in the central layers of a star under the conditions of the extremely high density. In order to stop the collapse and to support the explosion, the neutrinos have to be transported fast to the bounce shock. Our theoretical results confirm the idea that a large-scale convection should be the main transport mechanism for the neutrinos in SNe II. Large convective bubbles drift the high-energy neutrinos to the outer layers of the star, where they finally escape and reach the bounce shock.

The explosion of SN 1987A is of considerable interest for modern fundamental physics, both the physics of elementary particles and modern theoretical astrophysics. This supernova exploded in the Large Magellanic Cloud in 1987, when astronomical instruments allowed observations over the entire electromagnetic spectrum, as well as instruments for neutrino detection were operating. Neutrino events were recorded by the IMB, Kamiokande II, LSD instruments and the Baksan telescope (Bionta et al. 1987, Hirata et al. 1987, Aglietta et al. 1987). The LSD signal was detected five hours earlier than the other signals. Though models explaining this delay were subsequently suggested, a completely consistent model is still lacking.

The presence of a neutrino burst was interpreted as an indication of the gravitational collapse of the massive stellar core, forming a compact remnant – neutron star or black hole. Several papers in the early 1990s claimed that we would see the neutron star in the next three to five years, after the expansion of the envelope. However, no evidence of the presence of a compact remnant has been found more than 25 years after the outburst.

Another remarkable feature of this supernova is early detection of lines of ^{56}Co , which is created in the central region of the outburst (Syunyaev et al. 1987, Shigeyama et al. 1987). A proposed model describing the transport of cobalt from the interior by convection was not confirmed in numerical computations. This early appearance of ^{56}Co lines could be explained by either an asymmetric explosion or by the complete disruption of the star (Chechetkin et al. 1980, 1988).

One of the main methods used to study newborn neutron stars is the detection of X-rays emitted during the accretion of matter from the envelope left behind. The upper limit for the X-ray flux from a point source in the SN 1987A remnant established by the Chandra space observatory is $5.5 \cdot 10^{34}$ erg/s (Park et al. 2004). The intensity of the optical radiation measured with the Hubble Space Telescope doesn't exceed $8 \cdot 10^{33}$ erg/s [Graves et al. 2005]. Several explanations of very low radiation in presence of compact remnant were sug-

gested in paper by (Graves et al. 2005). The possible absence of a compact remnant is of great interest for the scientific community.

In this study we have computed the mass of matter remains in the neighborhood of a possible compact remnant in case of spherically symmetrical supernova explosion. We also have estimated accretion rate and X-ray luminosity for comparison with the observations of SN 1987A.

2. Hydrodynamics of SN explosion

We have used a polytropic model of a star with index $\gamma = 4/3$ which corresponds to Eddington standard model with purely radiative heat transport. The pressure in this case is determined by radiation. This assumption is valid only in the central hot core of a star. Initial configuration was calculated from the condition of hydrostatic equilibrium of non-rotating ideal gas sphere with a simple equation of state $P = \rho RT/\mu$, where the mean molecular weight was assumed as $\mu = 0.7$. We did not recompute gravity field assuming the explosion does not violate its initial spherically symmetric distribution. To construct the equilibrium initial profiles of density and temperature we take the central values $\rho_c \sim 762$ g/cm³ and $T_c \sim 1.96 \times 10^8$ K what corresponds to the realistic pre-supernova star model at the beginning of helium burning stage (Woosley et al. 2002).

Hydrodynamic simulations were performed with our own numerical code based on the Piecewise Parabolic Method on a Local stencil (PPML) (Popov et al. 2007, Popov 2012). The key PPML-procedure written on FORTRAN could be found in (Ustyugov et al. 2009). PPML is an improvement over the popular Piecewise Parabolic Method (PPM) suggested in (Colella et al. 1984) for compressible flows with strong shocks. PPM was implemented in many modern hydrodynamic codes and is widely used in computational practice now. The principal difference between PPM and PPML is the way how the interface values of the variables are computed between the adjacent cells. Instead of 4-point interpolation procedure in the standard PPM we have suggested to evolve them with time using the conservation property of Riemann invariants. Only local information within the left and the right cells is utilized to construct the interface values in this approach. The price for this is a double application of the Riemann solver procedure and a greater memory requirement for the storage of the boundary values from the previous time step, i.e. more computational capacity is required. However the method has demonstrated a high accuracy on both smooth and discontinued solutions. It could be more suitable for problems where the requirement of low dissipation is crucial.

There are two possibilities to simulate the SN explo-

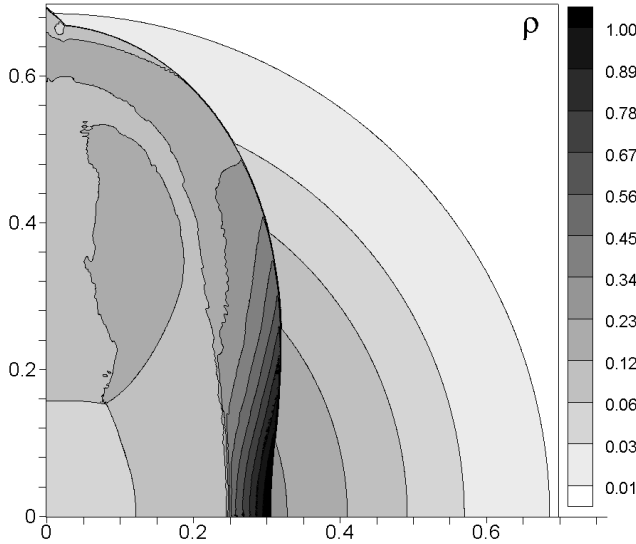


Figure 1: Density distribution for the moment $t = 19.5$ s after the inducing of the explosion. The coordinates are shown in the units of solar radius. Color represents the density in the units of $\rho_c = 762 \text{ g/cm}^3$.

sion: either by moving a piston as an inner boundary or depositing of the energy. Both of them involve free parameters. Piston is a time-dependent momentum deposition which requires the specification of the way how to move it (Woosley et al. 1995). It is easier to implement in Lagrangian hydrodynamics (mainly 1D) but the falling down matter could accumulate on the boundary reducing the accretion. The result yield is also sensitive to the mixing, fallback and explosion energy. In our SN model we use an alternative approach of the energy depositing to the central region of a star what is more natural for Eulerian hydrodynamics. As a parameter we need to define the size of the region where to insert the energy. The disadvantage of this approach is the possibility of the artificially entropy increase.

For numerical treatment we used a cylindrical coordinate system where all the variables depend on the vertical coordinate z and the distance r to z -axis, i.e. we assume rotational symmetry. Reflecting boundary conditions were imposed along the cylindrical axis and the equatorial plane, free outflow was allowed across the outer boundaries. We performed simulation in one quadrant with 800×800 grid resolution. We chose asymmetric explosion model "C" from (Maeda et al. 2002). The explosion energy $E \sim 1 \times 10^{52}$ ergs was divided between thermal and kinetic parts into two equal halves. The kinetic energy was distributed in an axisymmetric way by imposing different initial velocities in different directions: $v_z = \alpha z$ in the vertical direction and $v_r = \beta r$ on the equatorial plane. According to model "C" the ratio of the coefficients $\alpha : \beta = 8 : 1$. The energy E was deposit below $0.17 R_\odot$ radius which

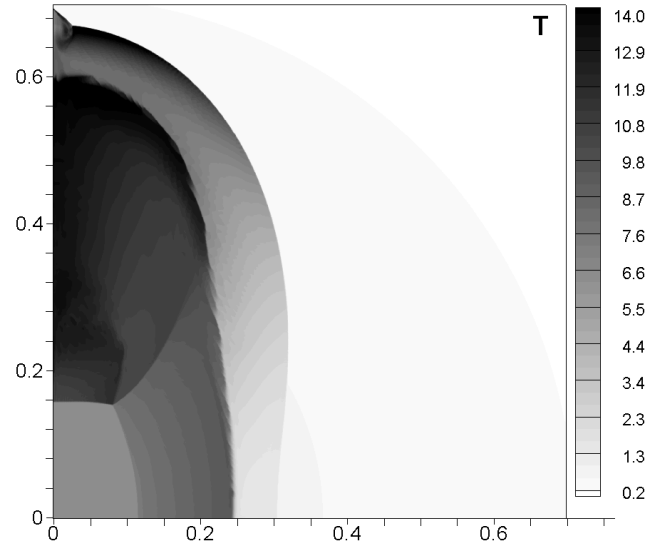


Figure 2: Temperature distribution for the same moment and in the same coordinate units as on fig. 1. Color represents the temperature in the units of 10^8 K .

contained $2 M_\odot$.

The simulation of supernova hydrodynamics with the initial parameters described above is presented on fig. 1-2 where the density and the temperature are shown respectively for the moment $t = 19.5$ s. The coordinates are in the units of solar radius. Color represents the density in the units of ρ_c and the temperature in 10^8 K . We detected a forward and a reverse shocks. The forward shock is moving up along the cylindrical axis, splitting into two shocks which are accelerating, entering into the lower density. This structure is tending to Sedov-Taylor self-similar solution when the energy of gravitational field becomes small comparatively to the kinetic energy of the expansion. The formation of the reverse shock in SNe models is a well known phenomenon, see for example (Couch et al. 2011, Gawryszczak et al. 2010). It forms on the distance $z \sim 0.2$ due to the resistance of the matter in front of propagating forward shock. The thrilling of the fronts near the cylindrical axis is a grid effect. Since in our model the most of the kinetic energy was introduced along the cylindrical axis, the motion in the equatorial plane is much less intensive (fig. 1). On fig. 2 you can see a bubble of hot matter which is formed between the reverse shock and the 'second' forward shock which is similar to the result obtained in (Couch et al. 2011). In this region the rates of the nuclear reactions must be most rapid.

3. Computations of compact remnant in SN explosion

To estimate the amount of ejected matter and matter that left in the vicinity of a compact remnant in

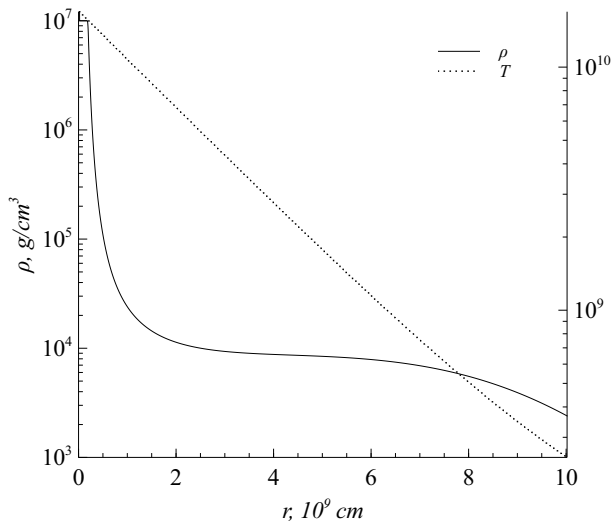


Figure 3: Initial distribution of density ρ and temperature T .

the process of the supernova outburst, we have computed the propagation of a shockwave through the pre-supernova shell. A gravitating object with mass $M_C = 1.35M_\odot$ and radius 10^7 cm was placed at the coordinate origin. This object corresponded to a proto-neutron star that was born as a result of the core collapse of the pre-supernova. It was surrounded by the envelope of helium with total mass around $15M_\odot$. The matter of the star shell was assumed as compressible non-viscous fluid. The generalized explicit Belotserkovskii–Gushchin–Kon’shin scheme (Belotserkovskii et al. 2005) was used to solve the set of hydrodynamical equations. For simplicity, explosion was assumed spherically symmetric, star was assumed non-rotating (only the radial velocity component is nonzero). Equation of state was one of the ideal gas with adiabatic index γ equals to $5/3$. Initial distribution of density and temperature were computed using hydrostatic equilibrium condition (see Fig. 3).

The shockwave was initiated by energy deposition in the $2 \cdot 10^7$ cm $< r < 2 \cdot 10^8$ cm spherical layer. Two kinds of energy deposition were used: positive radial velocity of $3 \cdot 10^7$ cm/s; and temperature jump by a factor of 10. The value of initial excitation was taken to provide kinetic energy of the shell of the order of 10^{51} ergs.

Calculations were performed on variable-scale grids. First the problem was solved in the range $2 \cdot 10^7$ cm $< r < 10^{10}$ cm. After the grid was changed by more rough one and external radius was increased up to 10^{13} cm. It was assumed that matter with velocity less than escape velocity will remain near the compact remnant and take part in subsequent accretion onto it.

Velocity profiles for different moments of time are presented on Fig. 4, together with escape velocity. It is seen from the figure that close to the center some

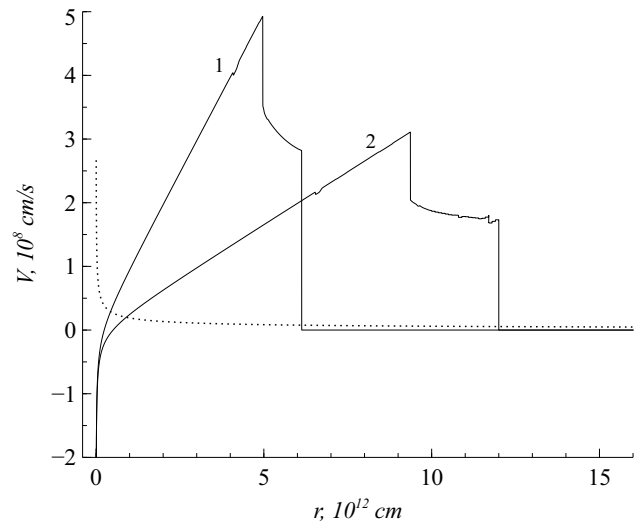


Figure 4: Velocity profiles for time of 1000 s (1) and 5000 s (2) after the outburst. The escape velocity is shown by dotted line.

part of matter has negative velocity. It shows that accretion has started.

One of the important results is the fact that after some time since the beginning of explosion ($2 \cdot 10^4$ s) matter of the envelope divides on two parts. The first part has velocity smaller than escape velocity. And total mass of this part is about $0.8M_\odot$ and remains constant (see Fig. 5). The outer boundary of this region expands with a decreasing velocity.

4. Estimation of accretion

The results of computations presented in the previous section show that more than $0.8M_\odot$ of matter in the envelope does not achieve the escape velocity, and forms the shell around the compact gravitating object. The next task was to evaluate the rate of accretion of remaining matter onto this object.

In the beginning we have performed rough estimates. To compute the rate of matter accretion, \dot{M} , onto the surface of the compact remnant of mass M , we used the formula for gas accretion from (Zeldovich and Novikov 1971):

$$\dot{M} = 10^{-14} \frac{\rho}{10^{-24} \frac{g}{cm^3}} \frac{M}{M_\odot} \left(\frac{V_\infty}{10 \frac{km}{s}} \right)^{-3}, \frac{M_\odot}{year}. \quad (1)$$

The accretion rate depends on the distribution of the matter density ρ in the envelope. However, for simplicity density was assumed to be uniform. It was derived from the size and mass of the remaining shell around the compact central object:

$$\rho = \frac{M_r}{4/3 \pi R_r^3}, \quad (2)$$

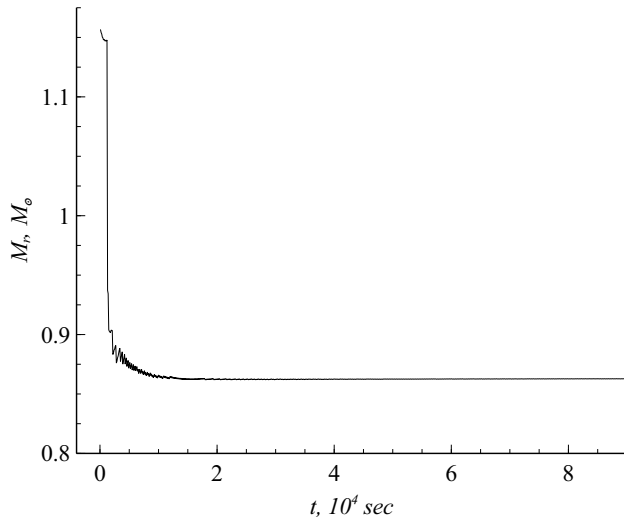


Figure 5: Mass of the compact shell M_r depending on time.

where M_r and R_r are the mass of the remaining shell and the maximum radius of its expansion; we treated R_r as parameter. For various values of R_r we have made estimation of accretion rate, lifetime of the shell and luminosity. The luminosity, L , was estimated by the formula:

$$L = \eta \dot{M} c^2, \quad (3)$$

where c is the speed of light and η is the efficiency of the transformation of the rest-mass energy into radiation, taken to be 0.1 (Graves et al. 2005). The results for various radii are presented in the Table 1.

Table 1: Luminosity L estimated for a uniform density distribution in the remaining shell.

R_r , cm	\dot{M} , M_\odot/year	Lifetime	L , erg/s
10^{14}	10^3	less than a day	10^{49}
10^{15}	1	~ 1 year	10^{46}
10^{16}	10^{-3}	10^3 years	10^{43}
10^{17}	10^{-6}	10^6 years	10^{40}
10^{18}	10^{-9}	10^9 years	10^{37}

The estimated luminosity is higher than is observed one by three orders of magnitude even for a radius of 10^{18} cm.

However, the physical problem is more complicated because of the non-uniform density profile along the radius. It is very difficult to perform a direct computation of the accretion for a time span of several years, starting from the beginning of explosion, because the velocity is very different in the neighborhood of the central object and at large radii.

The accretion rate was computed for a period about 20 hours starting from the outburst. The results are presented in Fig 6.

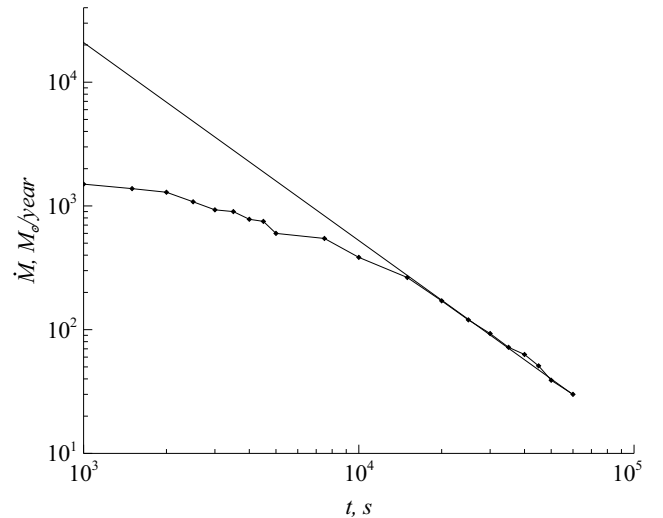


Figure 6: Accretion rate versus time since the outburst. The straight line is an extrapolation.

The accretion rate is fairly high at small times, but the computations show that it decreases with time. To estimate the accretion at later stages, we have extrapolated the accretion rate derived in our computations. The computations show that the decrease in the accretion rate is close to a power law:

$$\dot{M} = 1,37 \cdot 10^9 \left(\frac{t}{1s} \right)^{-1,6} M_\odot/\text{year}. \quad (4)$$

In this case, after ten years, when the envelope has certainly become transparent, the accretion rate drops to $10^{-5} M_\odot/\text{year}$. Following (Graves et al. 2005), the X-ray luminosity for this accretion rate is about 10^{40} erg/s. It is higher by six orders of magnitude than the observational upper limit of X-ray luminosity in the remnant of SN 1987A.

5. Conclusions

We have presented a simple approach for SNe modelization which allows to obtain a reliable picture of the explosion. The model is not overloaded with complicated physics and gives a clear understanding what is important and what could be neglected. More sophisticated models could be constructed against the background of this one. We did not compute self-gravity and used a simple equation of state. This is also not a full 3D simulation since we have assumed a rotational symmetry.

Our computations show that in case of supernova explosion with compact remnant (neutron star or black hole) significant amount of matter from the envelope remains in its vicinity. Computations were performed with parameters close to SN 1987A (mass of the progenitor and energy of explosion). The estimations of

spherical accretion presented in this paper indicate that X-ray luminosity after 10 years from explosion far exceeds the upper limits of luminosity from observations of the remnant of SN 1987A.

Acknowledgements. The computations were performed on LAPTH Cluster, Université de Savoie, France and on MVS-100K of Joint Supercomputer Center of the Russian Academy of Sciences. The work was supported by the Russian Foundation for Basic Research (project nos. 12-01-00606a, 12-02-00687a, 12-02-31737mol.a), Basic Research Programs no. 15 and no. 21 of the Presidium of the Russian Academy of Science and by the scientific school NSh-1434.2012.2.

References

- Aglietta M., Badino G., Bologna G., et al.: 1987, *IAU Cir.*, **4323**.
- Belotserkovskii O.M., Oparin A.M., Chechetkin V.M.: 2005, *Turbulence: New Approaches* (Cambridge International Science Publishing, Cambridge).
- Bionta R.M., Blewitt G., Bratton C.B., et al.: 1987, *Phys. Rev. Lett.*, **58**, 1494.
- Bychkov V., Popov M.V., Oparin A.M., Stenflo L., Chechetkin V.M.: 2006, *Astron. Rep.*, **50**, 298.
- Chechetkin V.M., Gershtein S.S., Imshennik V.S., et al.: 1980, *Astrophys. Space Sci.*, **67**, 61.
- Chechetkin V.M., Denisov A.A., Koldoba A.V., et al.: 1988, in *Supernova Remnants and the Interstellar Medium*, Ed. by R.S.Roger and T.L.Landecker (Cambridge, Cambridge University).
- Colella P., Woodward P.R.: 1984, *J. Comput. Phys.*, **54**, 174.
- Couch S.M., Pooley D., Wheeler J.C., Milosavljević M.: 2011, *Astrophys. J.*, **727**, 104.
- Gawryszczak A., Guzman J., Plewa T., Kifonidis K.: 2010, *A&A*, **521**, A38.
- Graves G.J.M.; Challis P.M., Chevalier R.A., et al.: 2005, *Astrophys. J.*, **629**, 944.
- Hirata K., Kajita T., Koshiba M., et al.: 1987, *Phys. Rev. Lett.*, **58**, 1490.
- Ivanova L.N., Imshennik V.S., Chechetkin V.M.: 1974, *Ap&SS*, **31**, 497.
- Khokhlov A.: 1991, *A&A*, **245**, 114.
- Maeda K., Nakamura T., Nomoto K., Mazzali P.A., Patat F., Hachisu I.: 2002, *Astrophys. J.*, **565**, 405.
- Moiseenko S.G., Bisnovaty-Kogan G.S., Ardeljan N.V.: 2010, *AIP Conf. Proc.*, **1206**, 282.
- Park S., Zhekov S.A., Burrows D.N., et al.: 2004, *Adv. Space Res.*, **33**, 386.
- Popov M.V., Ustyugov S.D., Chechetkin V.M.: 2004, *Astron. Rep.*, **48**, 921.
- Popov M.V., Ustyugov S.D.: 2007, *Comput. Mathem. & Mathem. Phys.*, **47**, 1970.
- Popov M.V.: 2012, *Comput. Mathem. & Mathem. Phys.*, **52**, 1186.
- Shigeyama T., Nomoto K., Hashimoto M., Sugimoto D.: 1987, *Nature*, **328**, 320.
- Syunyaev R.A., Kaniovskii A.S., Efremov V.V., et al.: 1987, *Sov. Astron. Lett.*, **13**, 431.
- Ustyugov S.D., Chechetkin V.M.: 1999, *Astron. Rep.*, **43**, 718.
- Woolley S.E., Weaver T.A.: 1995, *ApJS*, **101**, 181.
- Ustyugov S.D., Popov M.V., Kritsuk A.G., Norman M.L.: 2009, *J. Comput. Phys.*, **228**, 7614.
- Woolley S.E., Heger A., Weaver, T.A.: 2002, *Rev. Mod. Phys.*, **74**, 1015.
- Zeldovich Ya.B. and Novikov I.D.: 1971, *Gravitation Theory and Stellar Evolution*, (Moscow, Nauka) [in Russian].

LOW MISSING MASS, SINGLE- AND DOUBLE DIFFRACTION DISSOCIATION AT THE LHC

L. Jenkovszky^{1,2,a}, A. Saliı̄^{1,b}, J. Turóci^{3,c} and D. Himics^{3,d}

¹ Bogolyubov Institute for Theoretical Physics, National Academy of Sciences of Ukraine
UA-03680 Kiev, Ukraine

² Wigner Research Centre for Physics, Hungarian Academy of Sciences 1525 Budapest,
POB 49, Hungary

³ Uzhorod State University

^a jenk@bitp.kiev.ua, ^b saliı̄.andriy@gmail.com, ^c turoczi.jolika@citromail.hu, ^d himicsdia@hotmail.com

ABSTRACT. Low missing mass, single- and double diffraction dissociation is calculated for the LHC energies from a dual-Regge model. The model reproduces the rich resonance structure at low mass region, and approximate behavior for high mass-region.

1. Introduction

Measurements of single (SD) double (DD) and central (CD) diffraction dissociation (Dif.) are among the priorities of the Large Hadron Collider (LHC) at CERN.

In the past, intensive studies of high-energy diffraction dissociation were performed at the Fermilab, on fixed deuteron target, and at the ISR, see [1] for an overview and relevant references. One can see the rich resonance structure there, typical of low missing masses, often ignored by extrapolating this region by a simple $1/M^2$ dependence. When extrapolating (in energy), one should however bear in mind that, in the ISR region, secondary Reggeon contributions are still important (their relative contribution depends on momentum transfer considered), amounting to nearly 50% in the forward direction. At the LHC, however, their contribution in the nearly forward direction is negligible, i.e. less than the relevant error bars in the measured total cross section [3].

This new situation makes diffraction at the LHC unique in the sense that for the first time Regge-factorization is directly applicable.

2. Pre-LHC measurements: ISR, Fermilab and Tevatron (CDF)

Previous to the LHC, single diffraction dissociation was intensively studied at the ISR the Fermilab (fixed deuteron target) and at the Tevatron in the range of $14 < \sqrt{s} < 1800 \text{ GeV}$, $|t| < 2 \text{ GeV}^2$, and missing masses ranging from the threshold up to $\xi < 0.15$. The main results of these measurements and of their theoretical interpretation can be summarized as follows, for details see, e.g. [1, 2]:

1. Energy dependence. At the ISR and Fermilab energies the integrated SD cross section rises with s according to the standard prescription of the Regge-pole theory, however it slows down beyond. This effect was expected due to the familiar problem related to the violation of unitarity, namely that at high energies, implying the triple Pomeron limit, the D cross section overshoots the total cross section, $\sigma_{SD} > \sigma_T(s)$. Various means were suggested [5] to remedy this deficiency, including decoupling (vanishing) of the triple Pomeron vertex. Goulianos renormalizes the standard Pomeron flux to meet the data, see [2]. Such a “renormalization” produces a break near $\sqrt{s} \approx 20 \text{ GeV}$ slowing down the rise of $\sigma_{SD}(s)$ in accord with the CDF data from the Tevatron.

We instead will cure this problem by using rudiments of a dipole Pomeron (DP), compatible with unitarity without any renormalization factor, that produces a sharp (non-analytic) change in the behavior of $\sigma_{SD}(s)$: a dipole Pomeron (double Pomeron pole) is compatible with unitarity, in particular in the sense that both the SD cross section rises proportionally with the total cross section. The DP produces logarithmically growing cross sections at unit Pomeron intercept, however to meet the observed